ARTICLE

Temperature Effect on Hydrogen Evolution Reaction at Au Electrode

Zhi-qiang Tang, Ling-wen Liao, Yong-li Zheng, Jing Kang, Yan-xia Chen*

Hefei National Laboratory for Physical Sciences at the Microscale, Department of Chemical Physics, University of Science and Technology of China, Hefei 230026, China

The temperature dependence of hydrogen evolution reaction (HER) at a quasi-single crystalline gold electrode in both 0.1 mol/L HClO$_4$ and 0.1 mol/L KOH solutions was investigated by cyclic voltammetry. HER current displays a clear increase with reaction overpotential (η) and temperature from 278−333 K. In 0.1 mol/L HClO$_4$ the Tafel slopes are found to increases slightly with temperature from 118 mV/dec to 146 mV/dec, while in 0.1 mol/L KOH it is ca. 153±15 mV/dec without clear temperature-dependent trend. The apparent activation energy (E_a) for HER at equilibrium potential is ca. 48 and 34 kJ/mol in 0.1 mol/L HClO$_4$ and 0.1 mol/L KOH, respectively. In acid solution, E_a decreases with increase in η, from E_a=37 kJ/mol (η=0.2 V) to 30 kJ/mol (η=0.35 V). In contrast, in 0.1 mol/L KOH, E_a does not show obvious change with η. The pre-exponential factor (A) in 0.1 mol/L HClO$_4$ is ca. 1 order higher than that in 0.1 mol/L KOH. Toward more negative potential, in 0.1 mol/L HClO$_4$ A changes little with potential, while in 0.1 mol/L KOH it displays a monotonic increase with η. The change trends of the potential-dependent kinetic parameters for HER at Au electrode in 0.1 mol/L HClO$_4$ and that in 0.1 mol/L KOH are discussed.

Key words: Hydrogen evolution reaction, Au electrode, Temperature effect, Activation energy, Symmetric factor

I. INTRODUCTION

Hydrogen evolution reaction (HER) is of great importance for clean energy technologies such as water electrolysis and H$_2$ production [1−5]. Due to its simplicity, HER is also considered as one of the best model system for electrocatalysis. The effect of catalyst structure on the HER activity has been extensively studied in the past years, where a volcano plot between the rate for HER and the H adsorption energy at different metal substrates is well confirmed [6−8]. In acidic solution, three kinds of reaction mechanisms are proposed. The first step is believed to be the discharge of H$^+$,

$$H^+(aq) + e \rightarrow H_{ad} \qquad (1)$$

This is the so-called Volmer reaction. It may be followed by an electrochemical desorption step,

$$H_{ad} + H^+(aq) + e \rightarrow H_2 \qquad (2)$$
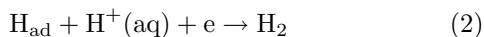
which is called Heyrovsky reaction. Or two adsorbed H atoms can combine and then desorb

$$H_{ad} + H_{ad} \rightarrow H_2 \qquad (3)$$

This step is called the Tafel reaction. Reaction going through steps (1) and (2) is called Volmer-Heyrovsky

mechanism, and reactions going through steps (1) and (3) is called Volmer-Tafel mechanism.

Among all metals studied for HER, Au electrode is found to have relative low HER activity. Studies with different single crystalline face of Au reveal that the HER activity decrease in the order of Au(100)-hex<Au(111)($\sqrt{3}$×22)<Au(110)(1×2)[6] [6], revealing that HER is a very structure sensitive reaction. HER at Au electrode is suggested to go through the Volmer-Heyrovsky mechanism [9], with the 1st step as rate determining step, however the details for the reactions mechanism are still unknown. Studying the temperature effect on HER kinetics will help to derive kinetic parameters, such as symmetric factor, activation energies and so on, which can provide useful information for the potential energies of the reactants and products along the reaction coordinates during HER. Such information will probably lead to much detailed understanding of HER mechanism as well as the factors which affect its reaction kinetics.

Temperature effects of several systems had been studied. Conway *et al.* obtained Tafel plots for the HER at Hg over a wide temperature range and differentiated the entropic and enthalpic components of the symmetry factor [10]. Kirowaeisner *et al.* reported the temperature-dependence of the transfer-coefficient for the HER at the dropping mercury electrode [11]. Temperature-dependence for the HER at solid gallium electrode had also been studied [12, 13]. While the temperature effect of HER at Au electrode have not yet been reported.

_____

*Author to whom correspondence should be addressed. E-mail: yachen@ustc.edu.cn, Tel.:/FAX: +86-551-3600035

In the present work, HER at a quasi-single crystalline gold electrode in both 0.1 mol/L HClO$_4$ and 0.1 mol/L KOH solutions were investigated by cyclic voltammetry over the temperature range of 278−333 K. Kinetic parameters, such as Tafel slopes, symmetric factors, exchange current density, activation energies and pre-exponential factor are derived. The mechanism for HER and the differences for HER at Au in 0.1 mol/L HClO$_4$ and 0.1 mol/L KOH are discussed based on the derived data.

II. EXPERIMENTS

The working electrode (WE) is quasi Au(111) single crystal surface (diameter: 2.5 mm). It was prepared from small bead, obtained by fusion and subsequent slow crystallization of Au wire of 0.8 mm in diameter (99.99%, Tanaka Noble Metal Corp.). After cooling, the resulting single crystal beads were oriented, cut and polished according to Clavilier's technique [14−16]. Prior to any experiment, the working electrodes were annealed for 10 s in a H$_2$+air flame, cooled in a reductive atmosphere (H$_2$+N$_2$), then quenched in ultra-pure water in equilibrium with this atmosphere. The electrode surface was covered by a water droplet to avoid contact impurities during transfer to the electrochemical cell and it was immersed into the solution under potential control, typically at 0.2 V (*vs.* SHE). A meniscus configuration was maintained between the Au surface and the electrolyte during all measurements.

A conventional three electrode cell was used in the present study, which was similar to the conventional cells used for RDE system [17], except for an additional glass jacket that allows circulating water around the cell for controlling the cell temperature. An Ag|AgCl (with saturated KCl solution) electrode and Au wire were used as reference (RE) and counter electrode (CE), respectively. The RE was placed in the second compartment to avoid the contamination of the solution by the leakage of Cl$^-$ or by traces of dissolved Ag$^+$ and also to keep it at room temperature (298 K). In this way, correction of the reference potential due to temperature changes was not required. All potentials in the work were quoted against reversible hydrogen electrode (RHE) at 298 K.

The electrolyte solution used in this study was 0.1 mol/L HClO$_4$ and 0.1 mol/L KOH, which was prepared using perchloric acid (70%, Sigma-Aldrich) and potassium hydroxide (99.99%, Sigma-Aldrich) and ultra-pure water (18.2 MΩ, Milli-Q pure water system). Before measurement at every temperature, continuous potential cycling in the potential region from 0.15 V to 1.7 V at a scan rate of 50 mV/s in electrolyte solution was carried out until the clean and reproducible cyclic voltammograms were obtained. Then, the electrode was washed carefully by ultra-pure water and immediately inserted into the cell filled with newly prepared solu-
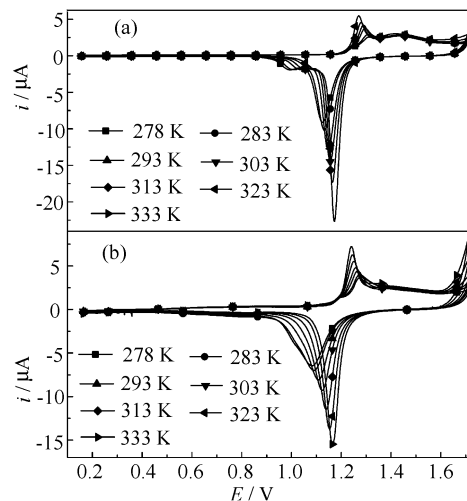

FIG. 1 Cyclic voltammograms of Au electrode in N$_2$ saturated (a) 0.1 mol/L HClO$_4$ and (b) 0.1 mol/L KOH at various constant temperatures, potential scan rate of 50 mV/s.

tions for basic cyclic voltammorgams (CVs) and HER measurements.

III. RESULTS AND DISCUSSION

A. Cyclic voltammetric characterization of Au electrodes and HER kinetics

Figure 1(a) displays the CVs of Au electrode in 0.1 mol/L HClO$_4$ at various constant cell temperatures, the general features of the CVs do not show obvious changes as the temperature of the electrolyte increases. From the CVs, it is seen that in the positive-going potential scan there is a broad double layer charging potential region from 0.3 V to 1.2 V, after that OH starts to adsorb on Au through the following reaction:

$$Au + H_2O \rightarrow Au–OH + H^+ + e \tag{4}$$
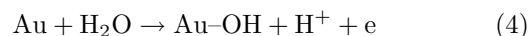
With further potential positive scan to above 1.3 V, the Au−OH is further oxidized to Au−O or AuO$_x$. With increase in cell temperature, it is seen that the current wave for Au−OH formation increases and its peak position shifts slightly negatively. In the negative-going scan from the positive limit of 1.7 V, Au−O$_x$ and Au−OH reduction begins at ca. 1.3 V and with a peak at around 1.1 V, which is followed by a small shoulder at in the potential region from ca. 0.9 V to 1.0 V. With increase in temperature, the peak potential for Au−O$_x$, Au−OH reduction shifts more positively and the peak width becomes narrower. This increase in sharpness can be attributed to the increase in reaction kinetics as the temperature increases.

The base CVs recorded in 0.1 mol/L KOH (Fig.1(b)) and their temperature dependence are largely the same as those in 0.1 mol/L HClO$_4$, except that the onset for
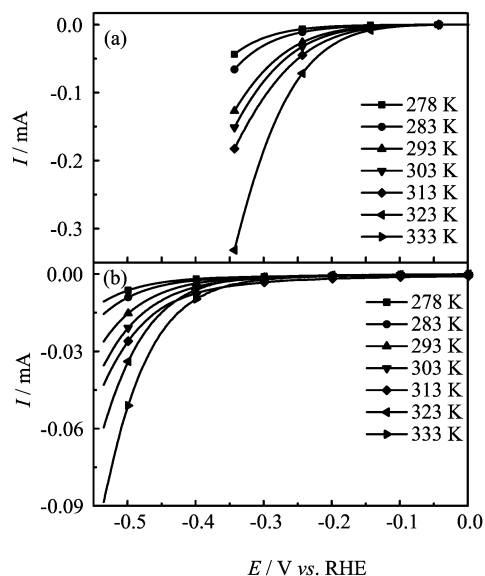
FIG. 2 Polarization curves for hydrogen evolution reactions at Au electrode in N_2 saturated (a) 0.1 mol/L $HClO_4$ and (b) 0.1 mol/L KOH at various constant temperatures, potential scan rate of 50 mV/s.

Au$-$OH formations is slightly negatively shifted on the RHE scale (ca. 50 mV). This is explained by the fact that in alkaline solution the formation of Au$-$OH is through the following reaction,

$$Au + OH^- \rightarrow Au\text{--}OH + e \qquad (5)$$

where breaking of O$-$H bond is not necessary, this is in contrast to the case in 0.1 mol/L $HClO_4$. Furthermore, in 0.1 mol/L KOH the Au$-O_x$ reduction displays a single broad peak rather than a sharp peak and a small shoulder in 0.1 mol/L $HClO_4$. The features shown in the base CVs are largely the same as those reported in Refs. [17, 18], suggesting that the cell system is clean. The overall reaction for hydrogen evolution at Au electrode in 0.1 mol/L $HClO_4$ is as the following:
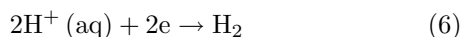
$$2H^+ \text{ (aq)} + 2e \rightarrow H_2 \qquad (6)$$

Figure 2(a) displays the polarization curves for HER in 0.1 mol/L $HClO_4$. From the figure, it is clearly seen that HER occurs at $E<$ca.-0.15 V at 278 K, and it shifts to positive potentials with the increase in cell temperature (e.g., the onset potential for HER is ca.-0.1 V at 323 K). At the same temperature, the HER current increases exponentially with the reaction overpotential, and at fixed potential the current displays an obvious increase with cell temperature, confirming that HER at Au electrode is an activated process.

The Tafel plots for HER in 0.1 mol/L $HClO_4$ at constant temperatures are displayed in Fig.3(a), from which the Tafel slopes are derived, which are given in Table I, from which it is seen that, in 0.1 mol/L $HClO_4$, the Tafel slopes is ca. 118.1 mV/dec at 278 K. And with
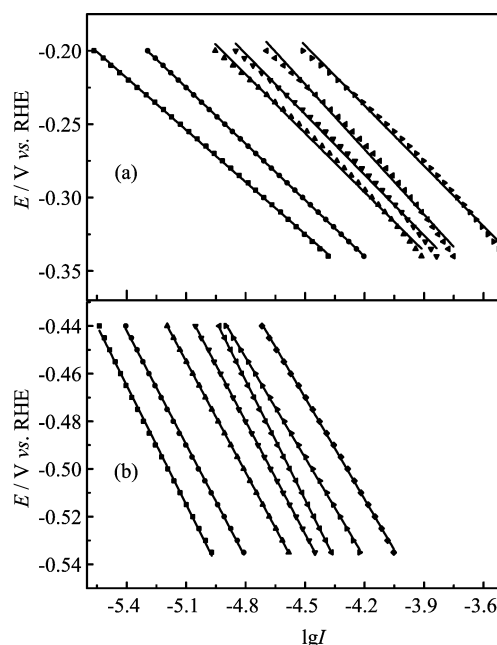
FIG. 3 Tafel plots for hydrogen evolution reactions at Au electrode in N_2 saturated (a) 0.1 mol/L $HClO_4$ and (b) 0.1 mol/L KOH at various constant temperatures of 278, 283, 293, 303, 313, 323, 333 K from left to right, raw data from Fig.2.

TABLE I Temperature dependence of the Tafel slopes and exchange current j_0 for HER at gold electrode in 0.1 mol/L $HClO_4$ and 0.1 mol/L KOH, j_0 is calculated using the data given in Fig.2 and using Eq.(4).

T/K	Tafel slope/(mV/dec)		j_0/(μA/cm^2)	
	$HClO_4$	KOH	$HClO_4$	KOH
278	118.1	167.7	1.1	1.4
283	128.1	159.8	2.8	1.5
293	133.3	155.4	7.5	1.9
303	137.6	157.4	10	2.8
313	146.7	167.5	19	5.5
323	136.0	139.7	22	18
333		141.4		29

increase in cell temperature, the Tafel slopes increases slightly. The values for the Tafel slopes for HER at temperatures close to room temperature determined in this study are in good agreement with that reported by Bockris et al. [19, 20] and Sasaki et al. [21, 22]. However, they are at variance with some other reports in Refs.[23–25]. Kuhn et al. [23] and Khanova et al. [24] observed two Tafel slopes, $2.3RT/2F$ at low current densities and $2\times2.3RT/F$ at high current densities. Conway et al. have also reported a Tafel slope of 60 mV/dec for the HER on polycrystalline gold at relatively low overpotentials [25]. In our experiment, the Tafel plots have only one value in a wide potential region especially at low temperatures, where very good
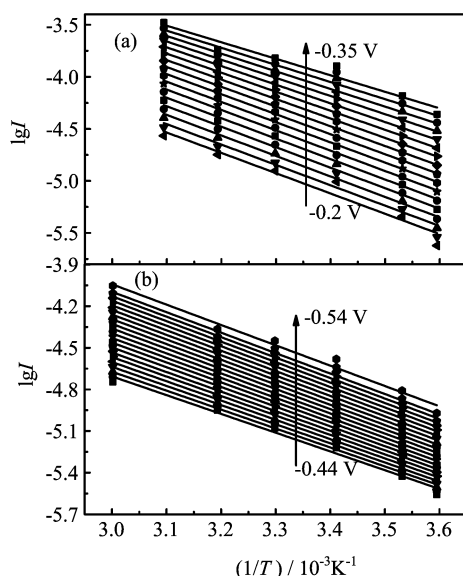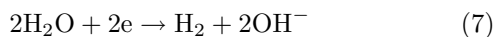
FIG. 4 Arrhenius plots for hydrogen evolution reactions at Au electrode in (a) 0.1 mol/L HClO$_4$ and (b) 0.1 mol/L KOH at various constant potentials, raw data from Fig.2.
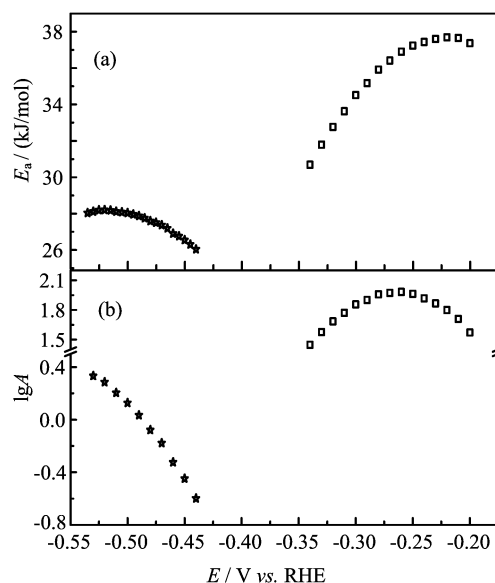

FIG. 5 Plots of (a) activation energies and (b) log of Arrhenius factor for hydrogen evolution reactions at Au electrode in 0.1 mol/L HClO$_4$ (right) and 0.1 mol/L KOH (left) as a function of reaction potential, data derived from Fig.4.

linear relationship exists (Fig.3).

Qualitatively, the HER behavior at Au in 0.1 mol/L KOH is quite similar to that in 0.1 mol/L HClO$_4$, except that the onset overpotential is ca. 0.15 V for HER through the following reaction:

$$2H_2O + 2e \rightarrow H_2 + 2OH^- \qquad (7)$$

which is higher than that through reaction in acidic solution. From the Tafel plots as given in Fig.3(b) and Table I, it is found that the Tafel slopes are ca. 160 mV/dec, which are slightly higher than those in acidic solution. The values (ca. 120 mV/dec to 160 mV/dec) of the Tafel slopes for HER in both acidic and alkaline solutions indicate that the rate determining step is the transfer of first electron in both solutions and it doesn't change with temperature.

B. Kinetic analysis of HER at Au electrodes

Using the original data for HER at Au electrode as given in Fig.2, the exchange current densities at different temperatures are derived according to the Butler-Volmer equation, where at overpotential lower than −0.12 V, the relationship between the overpotential and reaction current for HER can be expressed as follows:

$$j = j_0 \exp\left(-\frac{2\beta F\eta}{RT}\right) \qquad (8)$$

$$\eta = \frac{RT}{2\beta F}\lg j_0 - \frac{RT}{2\beta F}\lg j$$
$$= a - b\lg j \qquad (9)$$

where β is the symmetric factor for the rate determining step, j_0 is the exchange current density, b is the Tafel slope, R is gas constant, and T is temperature in Kelvin. The values for j_0 are given in Table I, it should be noted that the quasi-single crystalline Au electrode we used is rather smooth, its roughness factor should be less than 1.2 as may be deduced from the base CVs as given in Fig.1 for a disk electrode with diameter of 2.5 mm, thus the current density is deduced by normalizing the current to the geometric surface area. The exchange current density for HER at Au deduced in this study are in the order of μA/cm^2 range (Table I), it is ca. one order of magnitude higher than those at Au single crystalline electrode surface as reported by Kibler *et al.* [6] and by Perez *et al.* [26]. Since the quasi-single crystalline Au electrode we used is also rather smooth (RF<1.2), thus the one order of magnitude higher exchange current density may indicate that some defect sites at Au surface are much more active than the terrace sites toward HER.

The Arrhenius plots for hydrogen evolution reactions at Au electrode in both 0.1 mol/L HClO$_4$ and 0.1 mol/L KOH at various constant potentials are given in Fig.4. From which, the activation energies E_a and the pre-exponential factor A for HER at some selected potentials are obtained. E_a and $\lg A$ are plotted as a function of electrode potential shown in Fig.5 (a) and (b), respectively. E_a was found to decrease from 37 kJ/mol to 30 kJ/mol in overpotential region from 0.20 V to 0.35 V in 0.1 mol/L HClO$_4$, which is ca. 10 kJ/mol smaller than that at equilibrium potential. In contrast, in 0.1 mol/L KOH, E_a for HER at Au electrode is about 34 and 26 kJ/mol at η=0 and 0.44 V, which dis-
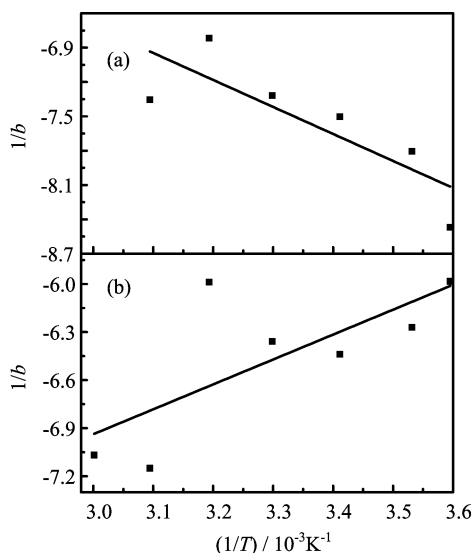
FIG. 6 Plots of reciprocal Tafel slopes $1/b$ *vs.* $1/T$ for hydrogen evolution reactions at Au electrode in (a) 0.1 mol/L HClO$_4$ and (b) 0.1 mol/L KOH, data derived from Fig.3.

plays slight increase (ca. 2 kJ/mol) with the increase in overpotential in the region from 0.44 V to 0.54 V. The potential-dependent trends for E_a of HER at Au electrode 0.1 mol/L HClO$_4$ to that in 0.1 mol/L KOH are just opposite to what has been found at Ag(111) and Ag(110) electrode in acidic solution at low and high overpotentials, respectively [27]. On the other hand, from Fig.5(b) it is seen that in 0.1 mol/L HClO$_4$, the lg$A$ is about 1.8±0.3. In 0.1 mol/L KOH, the lg$A$ displays a monotonically increase with the overpotential in the investigated potential range.

The change in the trends of the potential dependent E_a for HER at Au electrode 0.1 mol/L HClO$_4$ to that in 0.1 mol/L KOH may originate from the different temperature dependence of transfer coefficient. From the equation $\beta=\beta_H+T\beta_S$ proposed by Conway *et al.* [10], the reciprocal of the Tafel slope can be written as

$$\frac{1}{b} = -\frac{F\beta_H}{2.3RT} - \frac{F\beta_S}{2.3R} \qquad (10)$$

Figure 6 displays the reciprocal Tafel slope $1/b$ obtained in both 0.1 mol/L HClO$_4$ and 0.1 mol/L KOH as a function of $1/T$, and the β_H and β_S are calculated according to the slope and interception, respectively. From which, the temperature-dependence of β in 0.1 mol/L HClO$_4$ can be expressed as $\beta=\beta_H+T\beta_S=0.47-7.2\times10^{-5}T$, when the temperature was set as 298 K, the contribution of $T\beta_S$ is only about −0.002 to the total β which is equal to 0.465, which means the symmetry factor can be thought to be constant for this system if the temperature region is not so wide. The nearly temperature-independent transfer coefficient is the same as the result reported by Hamelin *et al.* [28].

In contrast, the temperature dependence of β for the HER at Au electrode in 0.1 mol/L KOH can be expressed as $\beta=-0.31+2.3\times10^{-3}T$, which differs much from the situation in 0.1 mol/L HClO$_4$. Setting the temperature as 298 K, we can get $T\beta_S=0.69$ and $\beta=0.38$. According to transition state theory, the rate constant for HER may be expressed by:

$$k \propto C \exp\left(\frac{\Delta^{\neq}S}{R}\right) \exp\left(-\frac{\Delta^{\neq}H}{RT}\right) \qquad (11)$$

The potential dependence of enthalpy change ΔH and entropy change ΔS was given by β_H and β_S, we can deduce that the potential dependence of E_a and A can be attributed to the potential-dependent change of ΔH and ΔS, respectively. Such changes correlate well with the temperature-dependent change in β, *e.g.*, in 0.1 mol/L HClO$_4$, E_a decreases with overpotential and β_H has a positive sign ($\beta_H=0.47$). In 0.1 mol/L KOH, E_a increases with overpotential and β_H has a negative sigh ($\beta_H=-0.31$). On the other hand, the potential dependence correlates well with that of β_S, *e.g.*, in 0.1 mol/L HClO$_4$ pre-factor A changes little with potential and β_S is 7.2×10^{-5}, while in 0.1 mol/L KOH A increases sharply with overpotential and β_S is 2.3×10^{-3}, which is nearly two orders of magnitude higher than the β_S in 0.1 mol/L HClO$_4$.

In a word, the increases of HER kinetics in 0.1 mol/L HClO$_4$ toward negative potentials can be mainly attributed to the reduction of ΔH between reactants and activated complex, in contrast, in 0.1 mol/L KOH it is mainly due to the increasing ΔS. This may indicate that, in 0.1 mol/L HClO$_4$, the potential change mainly alters the energy of electron at the Fermi level which is involved in the reaction for the discharge of H$_3$O$^+$. In contrast, in the discharge of water 0.1 mol/L KOH may involve significant change in the structure of water network from the reactant to activated complex, which causes large entropy change.

It should be mentioned that in previous SERS studies at coinage metals by Chen *et al.* [29, 30], in HER potential region abnormally enhanced bending mode of water is observed in non-acidic solutions, and the SERS band intensity increases toward more negative potentials. The structure change of water molecules in the hydrogen-bonded water network (involving those to be dissociated for HER) may be responsible for both the enhanced SERS signal of the bending mode of water and the large potential-depdendent entropy change involved in HER. Further investigations are underway to understand the implications of such information on HER mechanism and its reaction kinetic behavior.

IV. CONCLUSION

Hydrogen evolution reaction at a quasi-single crystalline gold electrode in both 0.1 mol/L HClO$_4$ and 0.1 mol/L KOH solutions was investigated by cyclic

voltammetry in the temperature range of 278−333 K. A clear increase in HER current with reaction overpotential and temperature is observed. In 0.1 mol/L $HClO_4$ the Tafel slopes are found to increase slightly from 118.1 mV/dec to 136.0 mV/dec with temperature, while in 0.1 mol/L KOH it is ca.153±15 mV/dec without clear temperature-dependent trend. From which, the temperature-dependence of the transfer coefficient β can be expressed as $\beta = \beta_H + T\beta_S = 0.47 - 7.2 \times 10^{-5}T$ in 0.1 mol/L $HClO_4$ and $\beta = -0.31 + 2.3 \times 10^{-3}T$ in 0.1 mol/L KOH.

The apparent activation energy for HER E_a was found to decrease from 37 kJ/mol to 30 kJ/mol at overpotentials from 0.20 V to 0.35 V in 0.1 mol/L $HClO_4$, and it increases from 26 kJ/mol to 28 kJ/mol at overpotentials from 0.44 V to 0.54 V. The pre-exponential factor A is ca. 1 order higher than that in 0.1 mol/L KOH. Toward more negative potentials, in 0.1 mol/L $HClO_4$ the pre-exponential factor A changes little with potential, while in 0.1 mol/L KOH it displays a monotonic increase with η. The change in the trends of the potential dependent E_a for HER at Au electrode 0.1 mol/L $HClO_4$ to that in 0.1 mol/L KOH correlates well with the different temperature dependence of transfer coefficient. In 0.1 mol/L $HClO_4$ the potential induced changes in the activation energy may be probably due to the change in activation enthalpy for HER. In contrast, in 0.1 mol/L KOH, the potential induced changes of activation energy may mainly be due to the change the entropy in HER.

V. ACKNOWLEDGMENTS

[1] A. Doner, R. Solmaz, and G. Kardas, Int. J. Hydrogen Energy **36**, 7391 (2011).
[2] T. N. Veziroglu and F. Barbir, *Energy Technology and the Environment*, New York: Wiley, 2712 (1995).
[3] I. Herraiz-Cardona, E. Ortega, and V. Perez-Herranz, Electrochim. Acta **56**, 1308 (2011).
[4] K. A. Adamson, Energy Policy **32**, 1231 (2004).
[5] M. Granovskii, I. Dincer, and M. A. Rosen, J. Power Sources **157**, 411 (2006).
[6] L. A. Kibler, ChemPhysChem **7**, 985 (2006).
[7] E. Santos, A. Lundin, K. Potting, P. Quaino, and W. Schmickler, Phys. Rev. B **79** (2009).
[8] E. Santos, P. Hindelang, P. Quaino, E. N. Schulz, G. Soldano, and W. Schmickler, ChemPhysChem **12**, 2274 (2011).
[9] N. Pentland, J. O. Bockris, and E. Sheldon, J. Electrochem. Soc. **104**, 182 (1957).
[10] B. E. Conway, and D. F. Wilkinson, J. Electroanal. Chem. **214**, 633 (1986).
[11] E. Kirowaeisner, M. Schwarz, M. Rosenblum, and E. Gileadi, J. Electroanal. Chem. **381**, 29 (1995).
[12] K. Szabo and J. Mika, Magy. Kem. Foly. **93**, 495 (1987).
[13] K. Szabo and K. Vargapal, Magy. Kem. Foly. **99**, 219 (1993).
[14] J. Clavilier, D. Armand, S. G. Sun, and M. Petit, J. Electroanal. Chem. **205**, 267 (1986).
[15] J. Clavilier, R. Faure, G. Guinet, and R. Durand, J. Electroanal. Chem. **107**, 205 (1980).
[16] J. Clavilier, J. Electroanal. Chem. **107**, 211 (1980).
[17] Q. J. Chen, Y. L. Zheng, L. W. Liao, J. Kang, and Y. X. Chen, Sci. Sin. Chim. **41**, 1777 (2011).
[18] G. Vazquez-Huerta, G. Ramos-Sanchez, A. Rodriguez-Castellanos, D. Meza-Calderon, R. Antano-Lopez, and O. Solorza-Feria, J. Electroanal. Chem. **645**, 35 (2010).
[19] J. O. Bockris and R. Parsons, Trans. Faraday Soc. **44**, 860 (1948).
[20] R. Piontelli, U. Bertocci, G. Poli, G. Serravalle, N. Pentland, J. O. M. Bockris, and E. Sheldon, J. Electrochem. Soc. **105**, 752 (1958).
[21] T. Sasaki and A. Matsuda, Chem. Lett. J. Inst. Catal. Hokkaido Univ. **21**, 157 (1973).
[22] T. Sasaki and A. Matsuda, Chem. Lett. J. Inst. Catal. Hokkaido Univ. **29**, 113 (1981).
[23] A. T. Kuhn and M. Byrne, Electrochim. Acta **16**, 391 (1971)
[24] L. A. Khanova and L. I. Krishtalik, J. Electroanal. Chem. **660**, 224 (2011).
[25] B. E. Conway and L. Bai, Electrochim. Acta **31**, 1013 (1986).
[26] J. Perez, E. R. Gonzalez, and H. M. Villullas, J. Phys. Chem. B **102**, 10931 (1998).
[27] D. Eberhardt, E. Santos, and W. Schmickler, J. Electroanal. Chem. **461**, 76 (1999).
[28] A. Hamelin, L. Stoicoviciu, S. C. Chang, and M. J. Weaver, J. Electroanal. Chem. **307**, 183 (1991).
[29] Y. X. Chen and A. Otto, J. Raman Spectrosc. **36**, 736 (2005).
[30] Y. X. Chen, S. Z. Zou, K. Q. Huang, and Z. Q. Tian, J. Raman Spectrosc. **29**, 749 (1998).